THE JOURNAL OF PHYSICAL CHEMISTRY B

Article

pubs.acs.org/JPCB

Theoretical Prediction of the Complexation Behaviors of Antitumor Platinum Drugs with Cucurbiturils

Natarajan Sathiyamoorthy Venkataramanan,* Suvitha Ambigapathy,† Hiroshi Mizuseki, and Yoshiyuki Kawazoe

Institute for Materials Research (IMR), Tohoku University, 2-1-1, Katahira, Aoba-Ku, Sendai, Japan - 980 8577

Supporting Information

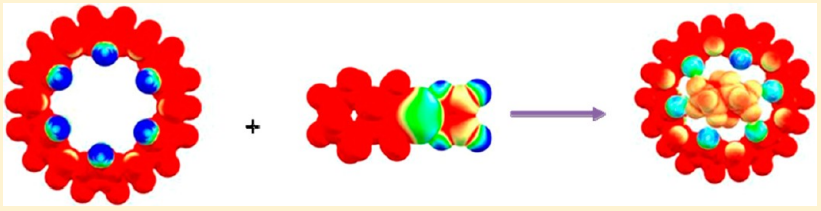

ABSTRACT: The inclusion complex formation ability between CB[*n*] (*n* = 6−9) and Pt-drugs (oxaliplatin, nedaplatin, carboplatin, and cisplatin) in gas phase as well as water phases has been investigated using the using density functional theory. The results reveal the existence of several stable inclusion complexes in aqueous solution with high solvation energies compared to the guest and host molecule. It has been shown that the formation of complexes between CB[6] and Pt-drugs resulted in structural change in the CB[6], with the calculated deformation energies being higher for the inclusion complexes. The inclusion complexes are stabilized by the hydrogen bonding and the charge transfer between the Pt-drugs and the CB[*n*] host. Calculated enthalpy and Gibbs free energy of formation in aqueous solution revels that the formation of CB[7]-oxaliplatin is spontaneous, and hence its experimental synthesis is feasible. Among the CB's studied, CB[8]−Pt-drug inclusion complexes have exothermic enthalpy and low Gibbs free energy of formation. Computed ^{1}NMR spectra in CB[7]−oxaliplatin showed high chemical shielding for the cyclohexane ring, indicating the existence of charge transfer in the inclusion complex. The amine protons in the guest Pt-drugs are shielded due to the hydrogen bonding interaction with CB's oxygen portal.

I. INTRODUCTION

Cisplatin, a widely known anticancer drug, is employed in chemotherapy against different kinds of solid tumors.[1,2] It is believed that DNA is the main target of cisplatin, and it can bind covalently to it producing distortions to the natural structure of the double helix. If enough of these adducts are produced without repair, the cell will die following an apoptotic process.[3−5] However, the above said process is not selective, and cisplatin interacts with noncancerous cells and other biomolecules producing secondary effects that limit the dose that can be administered.[6,7] In addition, some tumors are resistant toward the drug, and others can develop resistance after the treatment.[8] For the above reasons, a second generation of the drugs carboplatin (*cis*-diamminecyclobutane-1,1-dicarboxylateplatinum) and nedaplatin (*cis*-diammineglycolatoplatinum) were used in cancer treatment; however, in spite of the reduction of some side effects, when compared to cisplatin, they are still very reactive toward thiols that are present in the plasma proteins in the bloodstream and undergo degradation into nonactive complexes.[9]

Oxaliplatin (1,2-diaminocyclohexaneoxalateplatinum) is the recently FDA approved, third-generation anticancer platinium drug, which is active against some tumors that are primarily resistant to the other platinum compounds.[10] Furthermore, is the first antineoplastic agent to exhibit activity against metastatic colorectal cancer.[11] Recent research has shown that oxaliplatin is active in platinum-pretreated advanced ovarian cancer. It was hypothesized that oxaliplatin reaches DNA in the fully hydrolyzed form and forms adducts, which are more bulky and hydrophobic than those formed by the first- and second-generation platinum drugs, thereby inhibiting the DNA growth.[12] Further, they show higher lipophilicity, which is responsible for the more efficient removal from the blood through enhanced tissue penetration. Despite the success reached, several side effects including a reversible peripheral neuropathy characterized by paraesthesia and dysaesthesia in hands, feet, and the oral region were observed.[13] To circumvent the drawbacks of these FDA approved platinum(II)-based drugs, there has been a search toward new platinum drugs that include multinuclear and intercalating complexes.[14,15]

Macrocyclic host molecules have the potential to encapsulate biologically relevant guests and act as drug carriers, drug solubilizers, drug stabilizers, and drug bioavailability enhancers.[16,17] Encapsulation of drugs inside a macrocyclic host provides two benefits. First, it protects the drugs from degradation by steric hindrance to prevent the close approach

Received: October 4, 2012
Revised: November 18, 2012
Published: November 21, 2012

of nucleophiles, particularly glutathione and thiol or thiolate-containing proteins. Second, encapsulation can increase the specificity of the drugs for, and uptake into, cancerous cells, through the enhanced permeability and retention effect. This strategy has been extensively explored both for naturally occurring hosts such as cyclodextrins, as well as for synthetic molecular receptors such as calixarenes and crown ethers.[18,19]

A very promising emerging class of synthetic molecular hosts are cucurbit[n]urils (n = 5−8, 10). Cucurbit[n]urils (CB[n]) are macrocyclic cavitands with barrel-shape comprising glycoluril units.[20] Synthesis and structural analysis of CB[n] (n = 5−8, 10) have widely been investigated, while the formation of CB[9] occurs in minute amounts and hence is not isolated and well characterized. A CB[n] cavity is composed of two hydrophilic carbonyl-lined portrals capping a central hydrophobic cavity.[21] Further, the different sizes of the portals makes them capable of accommodating a variety of guests. A variety of organic drugs and biologically relevant molecules have been encapsulated in CB[n] including: ranitidine, aminoacids, cucurmin, amino anthracene, anthraquinones, pyrylium, and anticancer titanocene, ferrocene, and molybdocene compounds.[22−26] Their ability as potential stabilizing, solubilizing, activating, and delivering agents was also proved.[27,28]

Recently, Wheate and co-workers discovered that encapsulation of platinum drugs, with CB[n] allows the tuning of drug release rate and reduces the toxicity and degradation of the drug.[29,30] It was hypothesized that the binding efficiency of the platinum drugs decides their rate of degradation, while the size of CB[n], stability of the hydrolyzed aqua intermediate, and electronic factors decide the rate of their reaction with thiol or thiolate-containing proteins.[31,32] Several studies have been carried out to understand the nature of interaction of platinum drugs with CB[n].[33] An X-ray crystal structure of $PtCl_6$ with CB[7] has been documented, while NMR spectral studies on carboplatin with CB[7] shows absence of binding between the guest and host molecule.[34] Recently, Kim et al. established the existence of hydrophobic interaction between the oxaliplatin and CB[7] cavity though an X-ray crystal structure and ^{1}H NMR spectra.[35] Recently, in vivo studies have shown that cisplatin−CB[7] inclusion complex was found to be effective toward A2780/cp70 tumors, which are cisplatin resistant, which appears to be a pharamacokinetic effect.[36]

There exist many reports on the theoretical studies with CB[n]. Nau et al. made a MM+ force field optimization on the CB[6] molecule and reported a less symmetric collapsed structure, which presumably allows for some additional dispersion interactions between the walls without a significant increase in strain energy.[37] Later, Pichierri made a density functional theory (DFT) study on CB[n] (n = 5−10), and indicated that the macrocycles do possess D_{nh} symmetry.[38] Their thia analogues were also studied.[39] Zielesny and co-workers, made DFT investigation on the geometric, electronic, and NMR-shielding properties of CB[n] (n = 5 to 8), and reported that the molecules are highly symmetrical with a distinct geometric flexibility and a characteristic partial charge distribution.[40,41] Recently, Bakovest and co-workers made a thermodynamical analysis of macromolecule cyclization from a monomer to hexamer and found that water molecules, formed as one of the products, helps in the stabilization of the macrocycle.[42]

Gejji et al. made an assessment on the complex formation capability of CB[n] with ferrocene.[43] The host−guest complex formation of cucurbituril's with cation and anions, imidazole derivatives, and SF_6 were studied theoretically.[44−48] Using DFT, the inclusion formation ability of oxaliplatin with CB[n] (n = 5 to 8) was studied in gas phase, which shows that hydrogen bonding plays a major role in stabilizing the CB[7]-oxalplatin inclusion complex.[49] Reports on the complexation ability of cisplatin and nedaplatin were also carried out in gas phase.[50] However, during the experimental preparation of such inclusion complexes, solvent plays a major role in stabilizing the molecule.

In this work, we present a DFT study of the host−guest interaction between CB[n] (n = 6, 7, 8 and 9) with first-, second-, and third-generation Pt-drugs (oxaliplatin, nedaplatin, carboplatin and cisplatin) in gas as well as in aqueous phase. We focus our attention on the following: (i) Does CB[n] have the ability to accommodate Pt-drugs to form stable host−guest inclusion complex in gas phase as well as in aqueous phase? (ii) If so, what are the forces that are responsible for the formation of such stable complexes? (iii) Which are the inclusion complexes that are feasible to be prepared experimentally in aqueous solution? (iv) What are the common spectral techniques suitable for the identification of those inclusion complexes formed? This Article is organized as follows: Section II briefly describes the theoretical methods used in this work. In Section III, we first studied the structures and nature of interactions between CB[6] and Pt-drugs in gas phase. Then, the Gibbs free energy of formation for all inclusion complexes formed between CB[n] with Pt-drugs in aqueous phase were studied using the thermodynamic cycle. We have computed the ^{1}NMR chemical shifts for the protons to identify the complexes formed. Finally, the conclusions of the work are made in Section IV.

II. COMPUTATIONAL DETAILS

All the density functional theory calculations were performed with the Gaussian G09 program package.[51] Initial structure of CB[7]−, CB[8]−, and CB[7]−oxalipaltin were created from the reported X-ray crystal data.[35,52] The structural optimization were carried without any symmetry constraints using the hybrid B3LYP functional, composed of Becke's three-parameter hybrid exchange functional (B3) and the correlation functional of Lee, Yang and Parr (LYP).[53] The use of the hybrid B3LYP has been found to provide reliable results for the cisplatin and other platinum complexes.[54] In our previous study, the use of B3LYP functional provided accurate prediction of the bond parameters in comparison to the X-ray crystal data for the oxaliplatin−cucurbituril inclusion complex.[49] For the geometrical optimization of the studied complexes, we used the Los Alamos National Laboratory Lanl2DZ basis set.[55] The choice of B3LYP/Lanl2DZ for geometry optimization is justified as a compromise between reliable results and reasonable computational cost. To include the effects of water as a high-permittivity solvent, we used the CPCM method, with sphere radii optimized for COSMO-RS proposed by Klamt.[56] Test calculations were also done with UA0, UAHF, UAKS, and UFF cavities, and solution phase structure was compared with the X-ray crystal structure of CB[7]−oxaliplatin. This becomes essential as the solvation cavities largely alter the computed energies and properties. Our computed bond parameters with Klamt radii agree well with the reported X-ray crystal structure. In order to confirm the proper converges to minima and to evaluate the enthalpy of the reaction, vibrational frequencies were computed at the B3LYP/Lanl2DZ level of theory and

were confirmed to have no negative frequencies. Energies were computed using large basis set 6-311G(3d, 2p) basis set for all elements, while the Pt atom was described by the quasi-relativistic Stuttgart-Dresden pseudopotential (MWB-60) agumented by a set of diffuse (α_s = 0.075, α_p = 0.013, α_d = 0.025) and polarization functions (α_f = 0.98) for the valence orbitals.

The stabilization energy $E_{Stabiliz}$ was computed as the energy difference between the CB[n]−Pt complex [CB[n]−Pt$_{complex}$] and the individual compounds CB[n] and platinum complex. The strain energy E_{Strain} was computed from the energy differences between the total energy of the CB[n] molecule and that after the conformation deformation after the complexation of Pt-complex in solution. The reported energies in the text are basis set superposition corrected (BSSE). Partial charge analysis was done using the natural bond orbitals program (NBO) as implemented in the Gaussian 09 program at the B3LYP/Lanl2DZ level of theory in the CPCM solvation model.[57] Solvation free energies were computed with the use of the SMD model at the same level of theory using the Klamt radii on their respective solution-optimized geometries.[58] The Gibbs energy of formation in aqueous solution for the inclusion complexes was computed from the thermodynamic cycle

Scheme 1

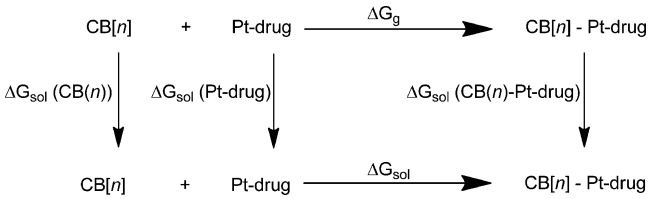

presented in Scheme 1. Thus, the Gibbs energy of formation in aqueous solution is calculated as

$$\Delta G_f = \Delta G_{gas} + \Delta G_{sol}(\text{CB}[n]\text{−Pt-drug}) - \Delta G_{sol}(\text{CB}[n]) - \Delta G_{sol}(\text{Pt-drug}) \quad (1)$$

where ΔG_{sol} is the solvation free energy. All of the thermochemistry computations were performed at standard conditions, that is, T = 298.15 K and P = 1 atm.

NMR chemical shifts (δ) were computed for the inclusion complexes in aqueous phase using self-consistent reaction field (SCRF) theory at the B3LYP level of theory by incorporating the CPCM model. The basis set 6-31G(d,p) was employed for C, H, N, O, and Cl and SDD basis set was used for Pt atom. The use of B3LYP/6-31G(d,p) has been reported to provide better chemical shifts for the CB[n] molecule.[41] Reported chemical shifts were obtained by subtracting the nuclear magnetic shielding tensors of protons in hosts and guests from those in the tetramethylsilane (as a reference) using the gauge-independent atomic orbital (GIAO) method.

II. RESULTS AND DISCUSSION

We have carried out a series of computations on the structure and electronic properties of CB[n]−Pt-drugs (n = 6,7,8 and 9) (Pt-drugs = cisplatin, carboplatin, nedaplatin and oxaliplatin) in the gas phase and aqueous solution. We have optimized the geometries of CB[n] (n = 6−9), and our results are consistent with the earlier experimental and modeling results.[35,38,47,52] As the complexation behavior between many Pt-drugs and CB[6] are unknown, we first studied the interactions of CB[6] with Pt-drugs (oxaliplatin, cisplatin, nedaplatin, and carboplatin) in all possible modes to understand the nature and stability for the formation of inclusion complexes. To determine the possible geometries of CB[6]−Pt-drug complexes, Pt-drugs were placed inside, on the top of the cavity and the side walls of CB[6] in different possible orientations and allowed to relax. The stable gas phase geometries of cisplatin, nedaplatin, oxaliplatin, and carboplatin with CB[6] are provided in Figure 1 and 2 with the important geometrical parameters at the B3LYP/Lanl2DZ level of theory in gas phase. The structures are arranged according to their lower stability compared with respect to the minimum energy structure. The structures are denoted with the notation A-CB[6]*x*, B-CB[6]*x*, C-CB[6]*x*, and D-CB[6]*x*, in which A, B, C, and D represent oxaliplatin, nedaplatin, carboplatin, and cisplatin, respectively, while "*x*" is the number of the structure. Further, we have studied the inclusion complexes of CB[n]-Pt-drugs for n = 7, 8, and 9 whose optimized structures and geometrical parameters are provided in the Supporting Information Figures S1 and S2 and Tables S1−S16.

A. Structure of CB[6]−Pt-Drug. Binding modes of oxaliplatin with CB[6] was studied by considering seven different modes that converge to five structures. The lowest-energy structure **A1** was the inclusion complex in which hydrogen atoms attached to the nitrogen of the oxaliplatin exist in hydrogen bonding with the ureidyl portal oxygen, with a N−H···O distance of 1.79 Å. The second lowest-energy isomer **A2** has the oxaliplatin in parallel orientation to the CB[6] ureidyl oxygen atoms. In **A2**, the hydrogen atoms attached to the nitrogen of the oxaliplatin exist in hydrogen bonding with the ureidyl oxygen, with a N−H···O distance of 1.83 Å. The **A3** structure has been predicted to be 91.7 kcal mol^{-1} higher in energy, in which the oxaliplatin's cyclohexane ring lies at a distance of 2.35 Å. The fourth lowest-energy isomer **A4** was the inclusion complex of oxaliplatin, which turns out to be 108.4 kcal mol^{-1} higher in energy, while in the **A5** structure the oxaliplatin interacting in the outer walls has the least stability. Structural comparison between inclusion complexes **A1** and **A4** shows that in **A4** the cyclohexyl rings provide high steric hindrance compared to the carbonyl group in **A1**, which stabilizes the **A1** conformer. The hydrogen bond distance between the CB[6]−oxaliplatin are depicted in Figure 1, from which one can understand that the hydrogen bonded interactions such as N−H···O or the C−H···O stabilized the complexation between the CB[6] and oxaliplatin.

Optimized geometries for CB[6]−nedaplatin are displayed in Figure 1 (see structures **B1**−**B4**). Six different initial configurations were attempted, which converges to four structures. The structure **B1** has the nedaplatin perpendicular to the upper rim ureidyl oxygen atoms. The −NH$_2$ substitute on the nedaplatin forms four hydrogen bond interactions with the upper rim oxygen atoms. In structure **B2**, the inclusion complex was also found to have four hydrogen bond interactions between the −NH$_2$ group of nedaplatin and the upper rim oxygen atoms, and was merely 1.7 kcal mol^{-1} higher in energy compared to the **B1** structure. Thus, we cannot confidently say which of the structures, **B1** or **B2**, was the lowest-energy structure, as the value is within the error of the theoretical method adopted. The third structure **B3** was found to have the nedaplatin in parallel orientation to the upper rim oxygen portal with two hydrogen bond interactions, and was 25.6 kcal mol^{-1} less stable than the lowest-energy structure.

dx.doi.org/10.1021/jp3098044 | J. Phys. Chem. B 2012, 116, 14029−14039

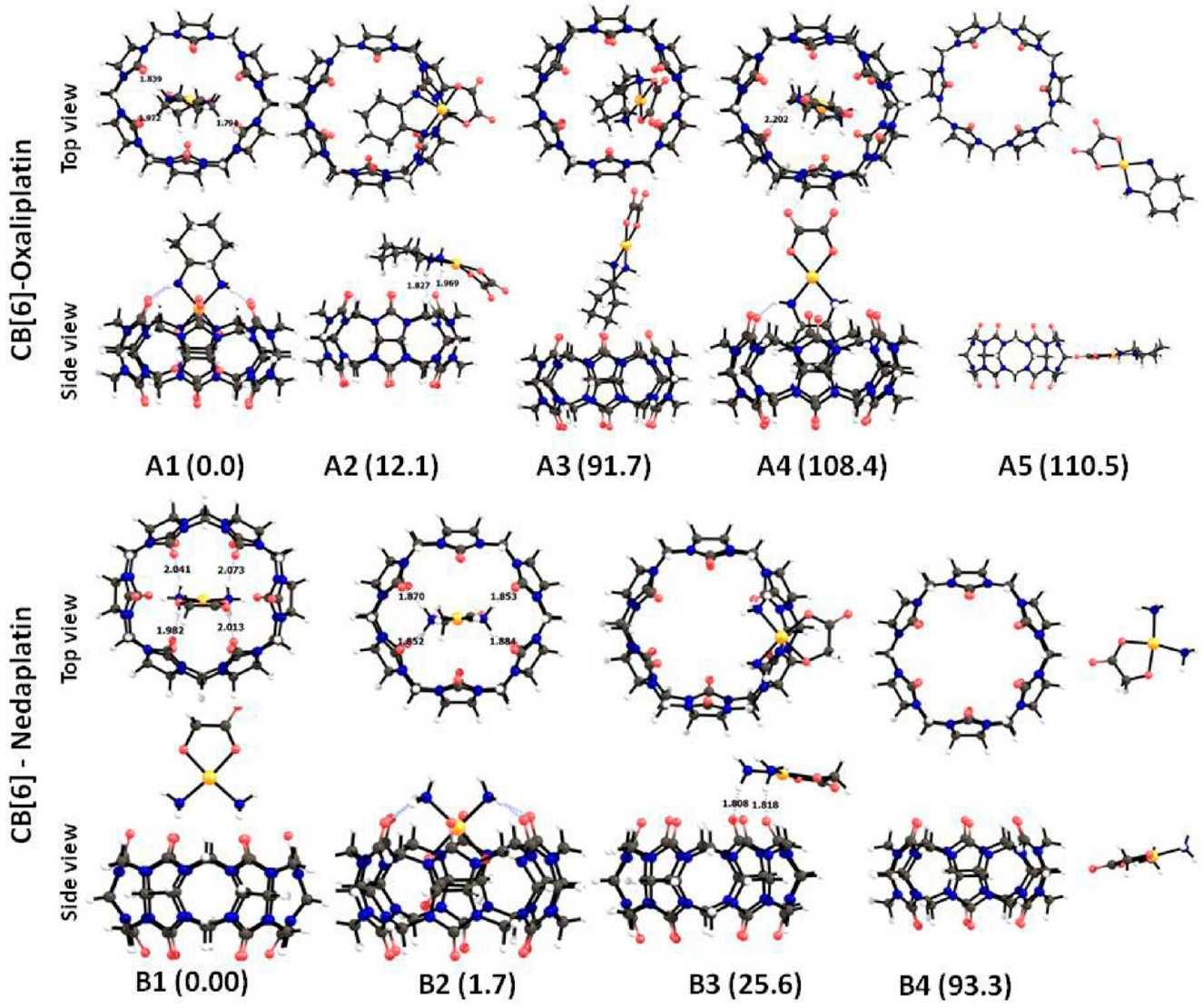

Figure 1. Optimized geometries of CB[6]−oxaliplatin and CB[6]−nedaplatin complexes from their side and top views.

The structure **B4** was found to be 93.3 kcal mol^{-1} less stable and has one hydrogen bond interaction between the carbonyl oxygen of the nedaplatin with the methylene hydrogen atom near the ureidyl oxygen of the CB[6].

On the attempted six different initial structures, the CB[6]−carboplatin complexes converge to four structures, **C1**−**C4**, which are presented in Figure 2. The lowest-energy isomer **C1** has the carboplatin on top and perpendicular to the CB[6] oxygen portal. The structure exists with four hydrogen bonds between the $-NH_2$ group of carboplatin and the upper rim oxygen atoms of the CB[6]. The second lowest-energy isomer **C2** was the one in which the carboplatin lies on top of the CB[6] and exists with two hydrogen bonding interactions. The third lowest-energy isomer was an inclusion complex **C3**, which is 63.7 kcal mol^{-1} higher in energy than the lowest energy isomer. The fourth isomer was the one in which the carboplatin exists at a nonbonding distance of 7.11 Å away from the CB[6], indicating carboplatin has weak interacting capability in the lateral orientation of CB[6].

For the cisplatin−CB[6] complexes, we have attempted five different initial structures, which converge to the three structures **D1**−**D3** that are depicted in Figure 2. The lowest-energy isomer **D1**, has the cisplatin in perpendicular orientation to the upper rim oxygen portal, with four hydrogen bonding interactions with the CB[6] molecule. The second lowest-energy isomer **D2** has two hydrogen bond interactions between the cisplatin and CB[6], in which cisplatin is oriented parallel to the upper rim oxygen portal. The inclusion complex **D3** was 25.7 kcal mol^{-1} less stable than **D1**. Thus the complexes with more hydrogen bonding interactions between the Pt-drug and the CB[6] are found to be the lowest-energy configurations. Similar arguments can be used to explain the energy lowering for the complexes **A1**, **B1**, and **C1** compared to their counterparts. On the other hand, lower stability of the inclusion complex **D3** is anticipated as the chlorine on the cisplatin is electronegative in nature, while the inner core of the CB[6] was highly electrodeficient.[59,60]

We then studied the inclusion complexes of CB[*n*]−Pt-drugs (*n* = 7, 8, and 9) by placing the Pt-drugs inside the cavity of CB[*n*] in all possible modes. The stable geometrical coordinates of the inclusion complexes are provided in the Supporting Information Tables S1−SX, and the number of hydrogen bonds that exist between the CB[*n*] and Pt-drugs in those inclusion complexes are provided in Table 3. The

dx.doi.org/10.1021/jp3098044 | J. Phys. Chem. B 2012, 116, 14029−14039

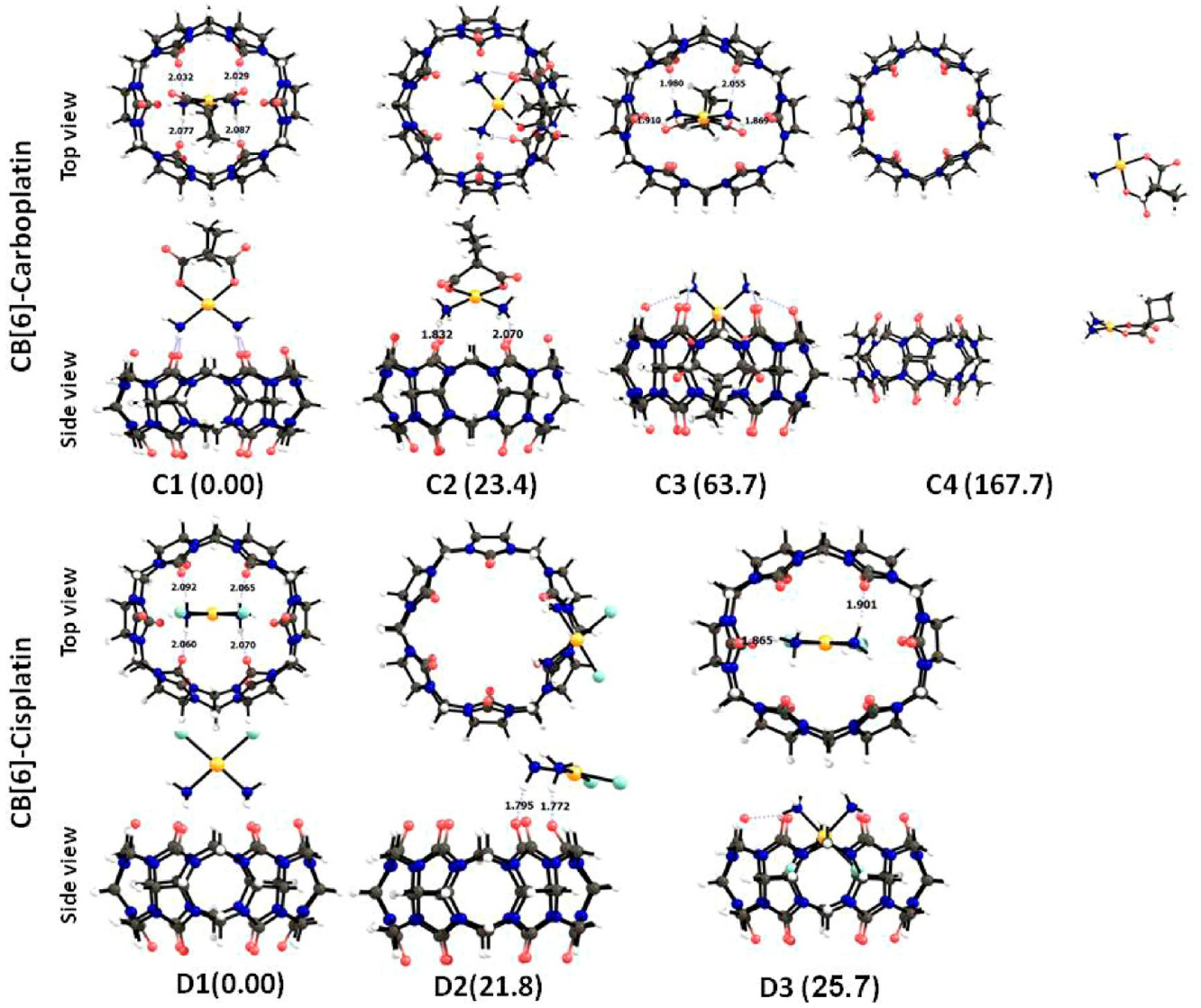

Figure 2. Optimized geometries of CB[6]−carboplatin and CB[6]−cisplatin complexes from their side and top views.

inclusion complexes formed between CB[n], n = 7, 8, and Pt-drugs are found to have the maximum number of hydrogen bonding between the upper rim ureidyl oxygen of CB[n] and hydrogen of Pt-drugs, whereas in CB[9], the Pt-drugs are attached to one end of the CB[9] ring due to its large portal diameter.

B. Energetic, Stability and Nature of Interaction. Calculated BSSE-corrected stabilization energies for all the complexes are reported in Table1. As may be inferred from Table 1, the studied complexes in different modes of interactions are stable except the **C4** complex, wherein the carboplatin exists at a nonbonding distance of 7.11 Å away from the CB[6]. Furthermore, the BSSE correction alters the stability of the **A1** and **A2** complex, making the inclusion complexes to be less stable for all the Pt-drugs. The stability of the inclusion complexes for the various drugs were in the order of oxaliplatin > nedaplatin > cisplatin > carboplatin. Thus, among the inclusion complexes, the carboplatin has the least interaction energy. It should be noted here that Wheate et al. were unable to find the interaction of such complexes with CB[7] in the NMR experiment.[34] Thus the present calculation supports the previous experimental findings.

A notable feature is the large structural change in the CB[6] host after its complexation with the guest Pt-drugs. The intramolecular distance between the oxygen portals are enlarged in one direction and are reduced in the perpendicular distance while accommodating the guest molecule. The calculated deformation energy on the CB[6] is comparably higher for the inclusion complexes. This shows that cucurbiturils are flexible hosts and could accommodate large guests. Meanwhile, the deformation energy of Pt-drug was higher for the inclusion complexes except the CB[6]−oxaliplatin system. In addition, the overall deformation energy was found to be low in the case of the CB[6]−oxaliplatin system. This implies that upon their complexation, they undergo much less structural reorganization. Furthermore, no regular trend has been observed between the stabilization energy, deformation energy, and the number of hydrogen bonds that exists between the Pt-drug and the CB[6] molecule. This shows the existence of addition stabilizing forces (*vide infra*) in addition to the hydrogen bonding between the host and the guest cucurbituril molecules.

In order to understand the addition forces existing in the inclusion complexes, we have calculated the NBO charges (see

dx.doi.org/10.1021/jp3098044 | J. Phys. Chem. B 2012, 116, 14029−14039

Table 1. Calculated Bond Parameters, Number of Hydrogen Bonds between Pt-Drug and CB[6], Deformation Energy, and Counterpoise Corrected Stabilization Energy $E_{Stabiliz}$ for the CB[6]−Pt-Drug Complexes in Gas Phase

structure	number of hydrogen bonds	shortest Pt-drug−CB[6] hydrogen bond distance	deformation energy (in kcal mol^{-1}) $E_{Def\text{-}Pt}$	deformation energy (in kcal mol^{-1}) $E_{Def\text{-}CB[6]}$	counterpoise corrected stabilization energy $E_{Stabiliz}$ (in kcal mol^{-1})
A1	3	1.839	(−6.03)[a] −1.85	(−16.47) −4.94	(−124.90) −54.25
A2	2	1.827	(−23.27) −6.14	(−10.20) −3.09	(−141.84) −56.70
A3	0		(−2.02) −0.520	(−1.93) −1.00	(−72.61) −43.58
A4	1	2.202	(−6.73) −1.18	(−13.88) −5.54	(−28.87) −24.17
A5	0		(−1.35) −0.05	(−2.58) −1.38	(−56.81) −41.49
B1	4	1.982	(−8.14) −1.25	(−16.31) −3.45	(−123.80) −43.91
B2	4	1.852	(−28.80) −5.91	(−12.38) −3.90	(−91.76) −48.42
B3	2	1.808	(−12.79) −2.84	(−5.69) −1.53	(−101.86) −59.91
B4	0		(−1.22) −0.168	(−1.93) −0.951	(−40.34) −33.21
C1	4	2.029	(−9.30) −1.43	(−17.85) −3.84	(−144.82) −39.51
C2	2	1.832	(−26.94) −4.55	(−31.56) −7.01	(−117.89) −54.26
C3	4	1.869	(−30.29) −5.25	(−40.01) −13.05	(−18.70) −12.15
C4	0		(−0.146) −0.091	(−0.328) −0.012	(3.47) −68.23
D1	4	2.060	(−5.09) −1.61	(−17.52) −3.73	(−136.46) −54.81
D2	2	1.772	(−10.23) −3.02	(−7.06) −1.91	(−115.57) −46.32
D3	2	1.865	(−35.15) −7.94	(−22.61) −7.51	(−77.05) −36.16

[a]Values in parentheses are from the B3LYP/Lanl2DZ level of theory.

Table 2. Calculated Solvation Energies, Enthalpy, and Gibbs Free Energies of Formation of Complexes and NBO Charges on Pt and Ligand in the CB[6]−Pt-Drug Complexes and Guest Pt-Drug in Aqueous Solution

structure	solvation energy in kcal mol^{-1}	enthalpy of formation in kcal mol^{-1}	Gibbs free energy of formation in kcal mol^{-1}	NBO Natural charge Pt	N	X	X1
oxaliplatin	−39.65			0.647	−0.826	−0.717	−0.717
A1	−24.09	−1.03	59.56	0.618	−0.845	−0.749	−0.750
A2	−63.99	−5.54	20.78	0.619	−0.830	−0.727	−0.728
nedaplatin	−25.62			0.572	−1.025	−0.750	−0.811
B1	−73.81	−5.58	0.771	0.546	−1.010	−0.753	−0.840
B2	−16.94	3.505	60.25	0.582	−1.030	−0.755	−0.839
carboplatin	−28.31			0.643	−1.013	−0.738	−0.738
C1	−74.39	−7.46	−1.56	0.606	−1.006	−0.751	−0.751
C3	−32.46	39.66	62.02	0.630	−1.026	−0.751	−0.755
cisplatin	−24.53			0.307	−0.995	−0.523	−0.523
D1	−71.78	−7.52	−0.66	0.268	−0.989	−0.545	−0.545
D3	−24.21	11.00	55.90	0.308	−1.002	−0.542	−0.542
cucurbituril[6]	−66.97						

Table 2) and plotted the molecular electrostatic potential (MESP) for the inclusion complexes. It is evident from Table 2 that NBO charges are high for the oxaliplatin and very low for the cisplatin. Upon complexation with CB[6], the charges on the metal atom decrease, which implies the gain in electron density by the Pt metal atom from the CB[6] molecule. On the other hand, the change on the amine nitrogen decreases except for the CB[6]−oxaliplatin system. Furthermore, the charges on the carbonyl oxygen comparatively remain the same in the case of nedaplatin and carboplatin inclusion complexes except the oxaliplatin−CB[6] inclusion complex.

It has been pointed out that the MESP diagrams are helpful in understanding the effective localization of electron density in the CB[n] molecular systems.[47,61] The MESP isosurface for the free and complexed Pt-durgs are shown in Figure 3. The electron rich regions are localized mainly on the ureidyl oxygen

dx.doi.org/10.1021/jp3098044 | J. Phys. Chem. B 2012, 116, 14029−14039

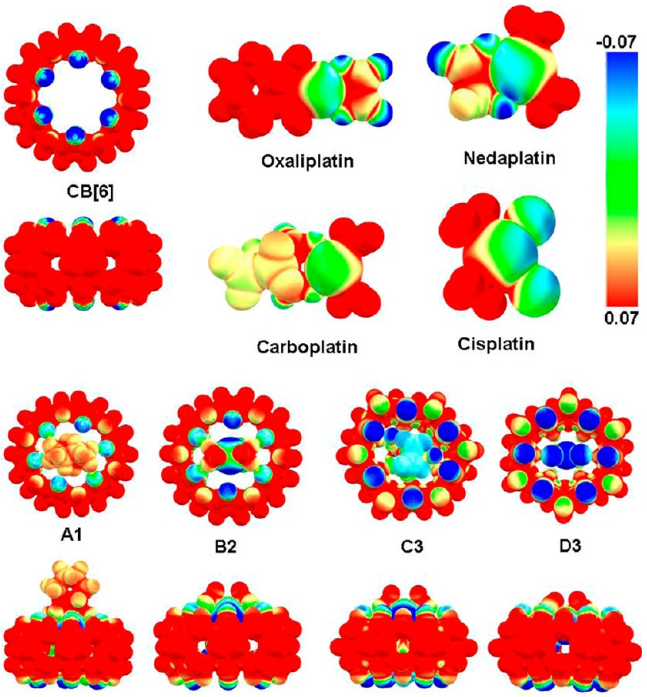

Figure 3. Selection of representative 3D MESP mapped on an electron density surface of 0.02 au. Scale of colors from red to blue represents MESP values ranging from −0.07 to +0.07.

atoms on the upper and lower rims of the CB[6] molecule. In the case of oxaliplatin, the cyclohexane part along with the amino group was found to be electron deficient, while the carbonyl groups are found to be electron rich. A similar trend has been observed in nedaplatin and carboplatin, in which the amine part was found to be electron deficient and the carbonyl groups are found to be electron rich. In the case of cisplatin, the amine group was found to be electron deficient, and the chloro groups are found to be electron rich. A comparison between bare Pt-drugs shows that oxaliplatin has a highly electron deficient part on the amino group. Among the inclusion complex, a high electron density transfer is observed from the ureidyl oxygen atom to the amino and cyclohexane part in the case of CB[6]−oxaliplatin. This explains the extra stability of the CB[6]−oxaliplatin complex compared to the other inclusion drugs. Thus, in addition to the hydrogen bonding, charge transfer plays a vital role in the stabilization of Pt-drugs inside the CB[*n*] cavity.

C. Formation of CB[*n*]−Pt-Drug in Aqueous Media. Understanding the solubility and formation thermodynamics of CB[*n*]−Pt-Drug in aqueous media is essential to design new drugs, as the new drug should have absolute solubility and high permeability toward the infected cells.[62,63] Furthermore, recent isothermal titration and molecular dynamics simulation studies illustrate the release of high-energy water from the cavity of CB[*n*] during its complexation with neutral guests in aqueous solutions.[64] Hence we have computed the solvation energy and Gibbs free energy of formation using the thermodynamic cycle shown in Scheme 1, for the CB[*n*] (*n* = 7, 8 and 9) inclusion complex and for the complex with high stabilization energy. The calculated parameters in aqueous media for the Pt-drug, CB[*n*], and inclusion complex are provided in Tables 2 and 3. Among the Pt-drugs studied, oxaliplatin has the high solvation energy, and nedaplatin has a very low solvation energy. This implies that oxaliplatin can more readily be dissolved in water compared to other Pt-drugs. The calculated solvation energy of CB[*n*] reveals that CB[9] has high solvation energy. Furthermore, odd numbered CB's have higher solvation energies than the even numbered CB's. It is worth pointing out here that our predications are in line with the previous studies on the solvation of CB[*n*] (*n* = 6,7, 8 and 10) in water in which CB[7] has experimentally high dissolution in water.[34]

Among the Pt-drug−CB[6] complexes, inclusion complexes are found to have low solvation energy. This is expected in view of the fact,that inclusion complexes would have low surface area to interact with water molecules compared to the hydrogen-bonded association complexes formed between Pt-drug and CB[6]. Furthermore, the complexes **A2**, **B1**, **C1**, and **D1**, which are formed by association of Pt-drug with CB[6], have higher solvation energy than the pristine CB[6] molecule. From Table 2, it is evident that the solvation energy for the various Pt-drug-inclusion complexes are much lower than that of the CB[6] molecule and are in the order carboplatin > cisplatin >

Table 3. The Number of Hydrogen Bonds Between the Guest and Host Molecule in the Inclusion Complex, Calculated Solvation Energies, Enthalpy, and Gibbs Free Energies of Formation for the CB[*n*]−Pt-Drug (*n* = 7, 8 and 9) Complexes in Aqueous Solution

CB[*n*]	Pt-drug	number of hydrogen bonds between CB[*n*] and Pt-drug	solvation energy in water (kcal mol^{-1})	enthalpy of formation in aqueous solution (kcal mol^{-1})	Gibbs free energy of formation in aqueous solution (kcal mol^{-1})
CB[7]			−79.33		
	oxaliplatin	4	−99.46	−37.08	−0.590
	nedaplatin	4	−5.10	−10.77	87.33
	carboplatin	4	−2.56	−20.65	84.85
	cisplatin	4	−7.56	−9.73	80.73
CB[8]			−49.93		
	oxaliplatin	3	−14.58	−6.57	31.05
	nedaplatin	4	−14.89	−26.52	23.86
	carboplatin	4	−14.02	−30.26	26.04
	cisplatin	4	−18.03	−19.31	27.54
CB[9]			−71.41		
	oxaliplatin	3	−43.80	−6.78	59.48
	nedaplatin	3	−43.29	−23.97	48.32
	carboplatin	4	−26.30	−31.27	63.54
	cisplatin	4	−40.86	−22.86	49.45

dx.doi.org/10.1021/jp3098044 | J. Phys. Chem. B 2012, 116, 14029−14039

oxaliplatin > nedaplatin. Among the inclusion complexes, the CB[6]−carboplatin inclusion complex will have the highest solubility in water, while the CB[6]−nedaplatin inclusion complex has the least solubility in water.

The computed solvation energy for the inclusion complexes of Pt-drug and CB[n] (n = 7, 8, and 9) are provided in Table 3. From Table 3, it is evident that CB[7] and CB[9] inclusion complexes have high solubility. Furthermore, no regular trend has been observed on the solvation ability of inclusion complexes based on the CB[n]. On the basis of the computed solvation energies the inclusion complex CB[7]-oxaliplatin has the highest solvation energy and CB[7]-carboplatin have the least solubility in water.

Gibbs formation energies in aqueous solution have been obtained from the thermodynamic cycle presented in Scheme 1. The relevant data and the calculated formation enthalpies in aqueous solution for CB[6]−Pt-drugs and CB[n]−Pt-drugs (n = 7, 8, and 9) are summarized in Tables 2 and 3, respectively. Our calculations demonstrate in CB[6]−Pt-drug that the enthalpy of formation of hydrogen-bonded association complexes **A2**, **B1**, **C1**, and **D1** are exothermic in aqueous solution. Among the inclusion complexes, only **A2**, CB[6]−oxaliplatin, was found be exothermic during its formation in aqueous solution, whereas, in the case of inclusion complexes of CB[n]−Pt-drugs (n = 7,8 and 9), their formation is exothermic, and among them CB[7]−oxaliplatin was found to be highly exothermic with an enthalpy of −37.07 kcal mol^{-1}. In the case of nedaplatin inclusion complexes, the CB[8]−nedaplatin complex has the highest exothermic enthalpy of −26.51 kcal mol^{-1}. However, for the carboplatin and cisplatin cases, the inclusion complexes formed with CB[9] have the highest exothermic enthalpy.

Our computed Gibbs formation energies in solution reveals that the formation of inclusion complex by Pt-drugs with CB[6] is endergonic, whereas the hydrogen-bonded association complexes between carboplatin and CB[6] are exergonic in nature. In the case of other CBs, the formation of CB[7]−oxaliplatin has an exergonic energy of −0.590 kcal mol^{-1}, while the formation of the other inclusion complexes have endergonic energy. A comparison between the Gibbs formation in energy between CBs shows that CB[8] inclusion complexes have low endergonic energy. Thus our computation predicts that, inclusion complex formation in aqueous solution is spontaneous in the cases of CB[7]−oxaliplatin, and hence their experimental synthesis is feasible, while the formation of the CB[8] inclusion complex has a low endergonic Gibbs free energy of formation. Furthermore, the formation of cucurbituril−carboplatin inclusion complexes is not favored by high endothermic enthalpy and endergonic Gibbs free energy, which suggests that such a species may not be feasible experimentally.

D. Spectral Properties of Stable CB[n]−Pt-Drug Inclusion Complex in Aqueous Media. To provide information for the spectral characterization of the inclusion complexes, we have calculated vibrational frequency and ^{1}HNMR chemical shifts of the inclusion complexes that are formed spontaneously with exothermic enthalpy and exergonic Gibbs free energy along with their respective guest and host system. The IR spectra of inclusion complexes of CB[7]−oxaliplatin along with the guest oxaliplatin molecule and host CB[7] molecule is provided in Figure 4. The IR spectra for the other stable inclusion complexes CB[8]−oxaliplatin, CB[8]−nedaplatin, and CB[8]−cisplatin along with their host and guest molecules are provided in the Supporting Information, Figure S3. As seen from Figure 4, and Figure S3, compared to the inclusion complex CB[n]−Pt-drug, IR signals of CB[n] are much stronger due to their much larger molecular weights. As a result, the guest molecules in the inclusion complexes are easily masked by the CB[n] spectral bands. Furthermore, the inclusion complexes have a superposition of host and guest molecule bands. As a result, IR techniques are not suitable for the spectral characterization of the inclusion complexes.

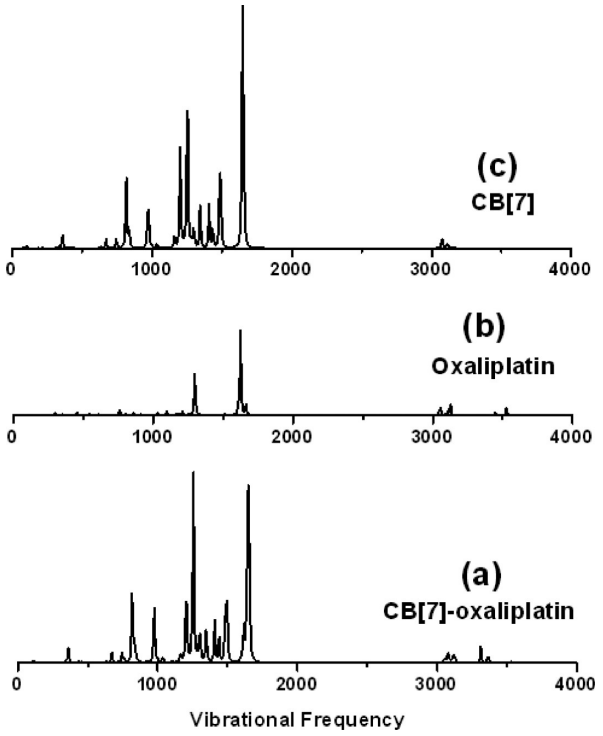

Figure 4. Calculated vibrational spectra of (a) CB[7]−oxaliplatin inclusion complex, (b) oxaliplatin host molecule, and (c) CB[7] guest molecule.

The calculated ^{1}H NMR spectra for CB[7]−oxaliplatin and CB[8]−oxaliplatin, along with the guest and host molecules are provided in Figure 5, while spectra of CB[8]−nedaplatin and CB[8]−cisplatin are provided in Figure S4 in the Supporting Information. The computed δ_H values for all the complexes, guest, and host molecules are provided in Supporting Information Tables S17−S20. In the CB[7] and CB[8] molecules, the methylene proton directing toward the ureidyl oxygen is largely deshielded and exhibits a downshift of δ_H 5.72 ppm and 5.73 ppm, respectively, while the other hydrogen attached to the methylene carbon has a δ_H value of 4.16 ppm and 4.14 pm. The hydrogen atoms attached to the carbon atoms located at the center and which are in the hydrophobic environment of the CB's have a δ_H value of 5.49 and 5.23 ppm. These values agree well with the experimental and theoretical values computed previously in aqueous solution.[65,47] The ^{1}H NMR spectra of guest molecule cisplatin shows two signals for the NH_3 molecules at 2.36 ppm and 2.28 ppm. In nedaplatin, the NH_3 protons show three signals positioned at 2.42, 2.22, and 1.87 ppm, whereas the methylene protons are positioned at 4.27 ppm. In the case of oxaliplatin, the NH_2 protons attached to the Pt atom are deshielded and exhibit a downshift to δ_H 3.12 ppm and 3.88 ppm, while the protons in the cyclohexane ring, which are nearer to the NH_2 groups, have a δ_H value of

dx.doi.org/10.1021/jp3098044 | J. Phys. Chem. B 2012, 116, 14029−14039

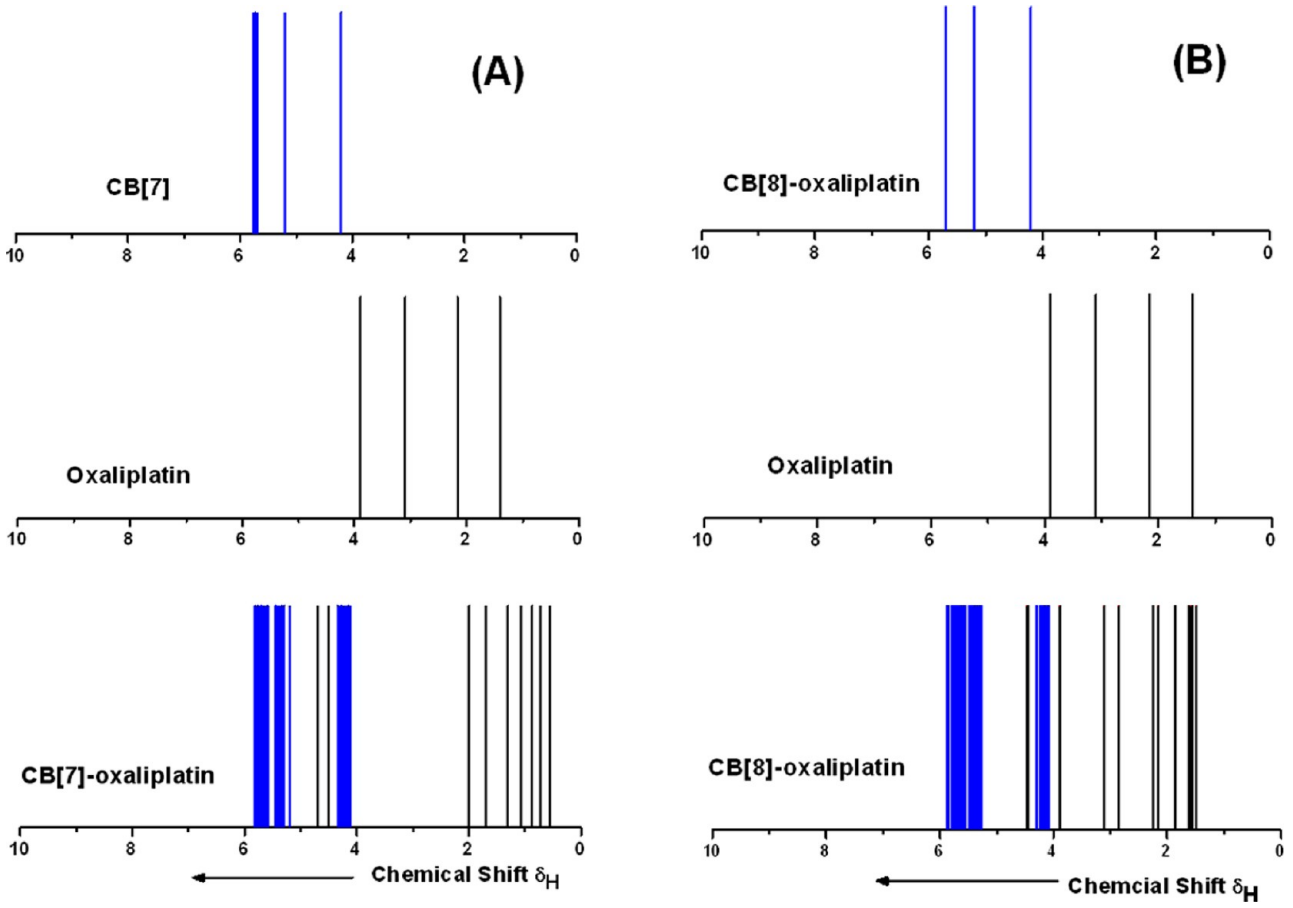

Figure 5. NMR Chemical shifts of the protons for (a) CB[7]−oxaliplatin, CB[7], and oxaliplatin and (b) CB[8]−oxaliplatin, CB[8], and oxaliplatin.

2.95 ppm, and the other protons in the ring have a δ_H value in the rage of 2.15−1.44 ppm.

^{1}H NMR spectra of the unbound oxaliplatin, CB[7], and the inclusion complexes CB[7]−oxaliplatin and CB[8]−oxaliplatin are depicted in Figure 5. To better visualize, the CBs' protons are shown in blue, while the guest molecules are provided in black. As can be readily noticed, the protons in the cyclohexane ring of oxaliplatin exhibit shielding upon encapsulation. The NH_2 protons in the oxaliplatin, which are in hydrogen bonding with the oxygen portal of the CBs, are shielded by about 1.3 ppm. However, in the case of the CB[8]−oxaliplatin inclusion complex, the NH_2 protons that are closer to the oxygen protons are more shielded than the other, which is due to the weak bonding of the other NH_2 protons. In the host molecule, the hydrogen atoms that are upward and near the ureidyl oxygen exhibit a deshielding by about 0.2 ppm. In CB[7]−oxaliplatin, the methylene protons in the hydrophobic part exhibit shielding by about 0.3 ppm. Similar results were observed experimentally for the CB[7]−oxaliplatin inclusion complex by Kim et al.; however, the observed signals were broad due to the fast exchange of protons on the NMR time scale and low signal-to-noise ratio, and hence a direct comparison was not made.[35] In the case of CB[8]−oxaliplatin, both deshielding and shielding were observed on the hydrophobic central part with those protons that are closer to the cyclohexene ring of oxaliplatin exhibiting shielding and those away from the cyclohexane ring being deshielded. This indicates that oxaliplatin forms a more stable inclusion complex with CB[7] due to its hydrogen boding and better change transfer ability compared to the CB[8] host. This result supports our previous finding in which oxaliplatin has the highest binding affinity for the CB[7] host among the CB[n] (n = 5, 6, 7, and 8).[49]

The calculated ^{1}NMR spectra of CB[8]−cisplatin and CB[8]−nedaplatin inclusion complexes along with the respective host and guest compounds are provided in Figure S4. The amine protons of cisplatin, which are hydrogen bonded, undergo a upfield shift by 0.9 ppm, while the other two protons undergo a deshielding and are observed at 3.61 ppm. The methylene protons that are in close proximity with ureidyl oxygen atoms and the hydrogen-bonded amine protons experience a deshielding, and those away from them experience a downfield shit. Due to the hydrogen bonding between ureidyl oxygen atoms and amine in cisplatin, the central hydrophobic methylene hydrogen atoms undergo an upfield shift in the ^{1}NMR spectra. A similar conclusion can be derived for the CB[8]−nedaplatin complex; however, the methylene protons on the nedaplatin undergo a shielding by 0.77 ppm.

IV. CONCLUSION

Extensive computational studies on the formation of inclusion complexes between CB[n] (n = 6−9) and Pt-drugs (oxaliplatin, nedaplatin, carboplatin, and cisplatin) reveal the existence of several stable inclusion complexes in aqueous solution with their formation driven by enthalpy and Gibbs free energy and are found to have high solvation energies compared to the guest and host molecule. We have studied the interactions of CB[6] with Pt-drugs in all possible modes to understand the nature and stability of the formation of the inclusion complexes

dx.doi.org/10.1021/jp3098044 | J. Phys. Chem. B 2012, 116, 14029−14039

formed. The formation of complexes between CB[6] and Pt-drugs resulted in structural change in the CB[6], with the calculated deformation energies being higher for the inclusion complexes.

Our computations showed that, in addition to the hydrogen bonding, charge transfer plays a vital role in the stabilization of Pt-drugs inside the CB[*n*] cavity. It has been observed that solvation energies of stable inclusion complexes are higher than their respective guest and host molecules. Calculated enthalpy and Gibbs free energy of formation in aqueous solution for the inclusion complexes are spontaneous in the cases of CB[7]−oxaliplatin. Among the CB's studied, CB[8]−Pt-drug inclusion complexes have exothermic enthalpy and low Gibbs free energy of formation. Normal vibration spectra of CB[*n*] are much stronger than the inclusion complex and Pt-drugs. Furthermore, the inclusion complexes have a superposition of host and guest molecule bands, and, hence, IR techniques are not suitable for the spectral characterization of the inclusion complexes. Computed ^{1}NMR spectra in CB[7]−oxaliplatin showed high chemical shielding for the cyclohexane ring, indicating the existence of charge transfer in the inclusion complex. The amine protons in the guest Pt-drugs are shielded due to the hydrogen bonding interaction with CB's oxygen portal. Thus, our findings would contribute to the design of new CB[*n*]−Pt-drug systems.

■ ASSOCIATED CONTENT

Supporting Information

Cartesian coordinate of the inclusion complexes between Pt-drugs and CB[*n*], ^{1}NMR chemical shifts for the stable inclusion complexes and IR and ^{1}NMR spectra of the stable inclusion complexes. This material is available free of charge via the Internet at http://pubs.acs.org.

■ AUTHOR INFORMATION

Corresponding Author

*E-mail: ramanan@imr.tohoku.ac.jp; nsvenkataramanan@gmail.com.

Present Address

[†]Department of Chemistry, Cauvery College of Engineering and Technology, Perur, Trichy, India - 639 103.

Notes

The authors declare no competing financial interest.

■ ACKNOWLEDGMENTS

The authors thank the crew of the Center for Computational Materials Science at Institute for Materials Research, Tohoku University, for their continuous support of the HITACHI SR16000 and SR11000 supercomputing facility.

■ REFERENCES

(1) Wang, D.; Lippard, S. J. *Nat. Rev. Drug Discov.* **2005**, *4*, 307−320.
(2) Kelland, L. *Nat. Rev. Cancer* **2007**, *7*, 573−584.
(3) Jamieson, E. R.; Lippard, S. J. *Chem. Rev.* **1999**, *99*, 2467−2498.
(4) Siddik, Z. H. *Oncogene* **2003**, *47*, 7265−7279.
(5) Roos, W. P.; Kaina, B. *Trends Mol. Med.* **2006**, *12*, 440−450.
(6) Reediijk. *J. Chem. Rev.* **1999**, *99*, 2499−2510.
(7) Borst, P.; Rottenberg, S.; Jonkers, J. *Cell Cycle* **2008**, *7*, 1353−1359.
(8) Martin, L. P.; Hamilton, T. C.; Schilder, R. J. *Clin. Cancer Res.* **2008**, *14*, 1291−1295.
(9) Montagnani, F.; Turrisi, G.; Marinozzi, C.; Aliberti, C.; Fiorentini, G. *Gastric Cancer* **2011**, *14*, 50−55.
(10) Stordal, B.; Pavlakis, N.; Davey, R. *Cancer Treat. Rev.* **2007**, *33*, 347−357.
(11) Hecht, J. R.; Patnaik, A.; Berlin, J.; Venook, A.; Malik, L.; Tchekmedyian, S.; Navale, L.; Amado, R. G.; Meropol, N. J. *Cancer* **2007**, *110*, 980−988.
(12) Saris, C. P.; vandeVaart, P. J. M.; Rietbroek, , R.C.; Blommaert, F. A. *Carcinogenesis* **1996**, *17*, 2763−2769.
(13) Wilson, R. H.; Lehky, T.; Thomas, R. R.; Quinn, M. G.; Floeter, M. K.; Grem, J. L. *J. Clin. Oncol.* **2002**, *20*, 1767−1774.
(14) Hall, M. D.; Hambley, T. W. *Coord. Chem. Rev.* **2002**, *232*, 49−67.
(15) Wheate, N. J.; Collins, J. G. *Coord. Chem. Rev.* **2003**, *241*, 133−145.
(16) Wheate, N. J.; Buck, D. P.; Day, A. L.; Collins, J. G. *Dalton Trans.* **2006**, *3*, 451−458.
(17) Garmann, D.; Warnecke, A.; Kalayda, G. V.; Kratz, F.; Jaehde, U. *J. Controlled Release* **2008**, *131*, 100−106.
(18) Dibama, H. M.; Clarot, I.; Fontanay, S.; Ben Salem, A.; Mourer, M.; Finance, C.; Duval, R. E.; Regnouf-de-Vains, J. B. *Bioorg. Med. Chem. Lett.* **2009**, *19*, 2679−2682.
(19) Nakahara, Y.; Okazaki, Y.; Kimura, K. *Soft Matter* **2012**, *8*, 3192−3199.
(20) Lee, J. W.; Samal, S.; Selvapalam, N.; Kim, H. J.; Kim, K. *Acc. Chem. Res.* **2003**, *36*, 621−630.
(21) Nau, W. M.; Florea, M.; Assaf, K. I. *Isr. J. Chem.* **2011**, *51*, 559−577.
(22) (a) Sindelar, V.; Parker, S. E.; Kaifer, A. E. *New. J. Chem.* **2007**, *31*, 725−728. (b) Wang, R. B.; Macartney, D. H. *Org. Biomol. Chem.* **2008**, *6*, 1955−1960.
(23) Buck, D. P.; Abeysinghe, P. M.; Cullinane, C.; Day, A. L.; Collins, J. G.; Harding, M. M. *Dalton Trans.* **2008**, *17*, 2328−2334.
(24) Thangavel, A.; Sotiriou-Leventis, C.; Dawes, R.; Leventis, N. *J. Org. Chem.* **2012**, *77*, 2263−2271.
(25) Thuery, P. *Inorg. Chem.* **2011**, *50*, 10558−10560.
(26) Lee, D. W.; Park, K. M.; Banerjee, M.; Ha, S. H.; Lee, T.; Suh, K.; Paul, S.; Jung, H.; Ki, J.; Selvapalam, N.; Ryu, S. H.; Kim, K. *Nat. Chem.* **2011**, *3*, 154−159.
(27) Appel, E. A.; Loh, X. J.; Jones, S. T.; Biedermann, F.; Dreiss, C. A.; Scherman, O. A. *J. Am. Chem. Soc.* **2012**, *134*, 11767−11773.
(28) Shen, C.; Ma, D.; Meany, B.; Isaacs, L.; Wang, Y. *J. Am. Chem. Soc.* **2012**, *134*, 7254−7257.
(29) Walker, S.; Kaur, R.; Mclnnes, F. J.; Wheate, N. J. *Mol. Pharmaceutics* **2010**, *7*, 2166−2172.
(30) Walker, S.; Oun, R.; Mclnnes, F. J.; Wheate, N. J. *Isr. J. Chem.* **2011**, *51*, 616−624.
(31) Wheate, N. J.; Day, A. L.; Blanch, R. J.; Arnold, A. P.; Cullinane, C.; Collins, J. G. *Chem. Commun.* **2004**, *12*, 1424−1425.
(32) Kemp, S.; Wheate, N. J.; Wang, S. Y.; Collins, J. G.; Ralph, S. F.; Day, A. L.; Higgins, V. J.; Aldrich-Wright, J. R. *J. Biol. Inorg. Chem.* **2007**, *12*, 969−979.
(33) Wheate, N. J.; Taleb, R. I.; Krause-Heuer, A. M.; Cook, R. L.; Wang., S.; Higgins, V. J.; Aldrich-Wright, J. R. *Daltron Trans.* **2007**, *43*, 5055−5064.
(34) Wheate, N. J. *J. Inorg. Biochem.* **2008**, *102*, 2060−2066.
(35) Jeon, J. J.; Kim, S.-Y.; Ko, Y. H.; Sakamoto, S.; Yamaguchi, K.; Kim, K. *Org. Bio. Chem.* **2005**, *3*, 2122−2125.
(36) Plumb, J. A.; Venugopal, B.; Oun, R.; Gomez-Roman, N.; Kawazoe, Y.; Venkataramanan, N. S.; Wheate, N. J. *Metallomics* **2012**, *4*, 561−567.
(37) Marquez, C.; Hudgins, R. R.; Nau, W. M. *J. Am. Chem. Soc.* **2004**, *126*, 5806−5816.
(38) Pichierri, F. *J. Mol. Struct.: THEOCHEM* **2006**, *765*, 151−152.
(39) Pichierri, F. *Chem. Phys. Lett.* **2004**, *390*, 214−219.
(40) Buschmann, H. J.; Wego, A.; Zielesny, A.; Schollmeyer, E. *J. Inclusion Phenom. Macrocyclic Chem.* **2006**, *54*, 85−88.
(41) Gobre, W.; Pinjari, R. V.; Gejji, S. P. *J. Phys. Chem. A* **2010**, *114*, 4464−4470.
(42) Bakovests, V. V.; Masliy, A. N.; Kuznetsov, A. M. *J. Phys. Chem. B* **2008**, *112*, 12010−12013.

(43) Pinjari, R. V.; Gejji, S. *J. Phys. Chem. A* **2008**, *112*, 12679−12686.
(44) Sundararajan, M.; Sinha, V.; Bandyopadhyay, T.; Ghosh, S. K. *J. Phys. Chem. A* **2012**, *116*, 4388−4395.
(45) Sundararajan, M.; Solomon, R. V.; Ghosh, S. K.; Venuvanalingam, P. *R. Soc. Ser. Adv. Sci.* **2011**, *1*, 1333−1341.
(46) Gupta, M.; Maity, D. K.; Singh, M. K.; Nayak, S. K.; Ray, A. K. *J. Phys. Chem. B* **2012**, *116*, 5551−5558.
(47) Dixit, P. H.; Pinjari, R. V.; Gejji, S. P. *J. Phys. Chem. A* **2010**, *114*, 10906−10916.
(48) Pinjari, R. V.; Gejji, S. P. *J. Phys. Chem. A* **2010**, *114*, 2338−2343.
(49) Suvitha, A.; Venkataramanan, N. S.; Mizuseki, H.; Kawazoe, Y.; Ohuchi, N. *J. Incl. Phenom. Macrocycl. Chem.* **2010**, *66*, 213−218.
(50) Nojini, Z. B.; Yavari, F.; Bagherifar, S. *J. Mol. Liq.* **2012**, *166*, 53−61.
(51) Frisch, M. J.; Trucks, G. W.; Schlegel, H. B.; Scuseria, G. E.; Robb, M. A.; Cheeseman, J. R.; Scalmani, G.; Barone, V.; Mennucci, B.; Petersson, G. A. et al. *Gaussian 09*, revision C.01; Gaussian, Inc.: Pittsburgh, PA, 2009.
(52) Kim, J.; Jung, I.-S.; Kim, S.-Y.; Lee, E.; Kang, J.-K.; Sakamoto, S.; Yamaguchi, K.; Kim, K. *J. Am. Chem. Soc.* **2000**, *122*, 540−541.
(53) (a) Becke, A. D. *Phys. Rev. A: At., Mol., Opt. Phys.* **1988**, *38*, 3098−3100. (b) Lee, C.; Yang, W.; Parr, R. G. *Phys. Rev. B: Condens. Matter Mater. Phys.* **1988**, *37*, 785−789. (c) Stephens, P. J.; Devlin, F. J.; Chabalowski, C. F.; Frisch, M. J. *J. Phys. Chem.* **1994**, *98*, 11623−11627.
(54) (a) Zimmermann, T.; Leszczynski, J.; Burda, J. V. *J. Mol. Model.* **2011**, *17*, 2385−2393. (b) Zimmermann, T.; Chval, Z.; Burda, J. V. *J. Phys. Chem. B* **2009**, *113*, 3139−3150.
(55) (a) Wadt, W. R.; Hay, P. J. *J. Chem. Phys.* **1985**, *82*, 270−283. (b) Wadt, W. R.; Hay, P. J. *J. Chem. Phys.* **1985**, *82*, 284−298. (c) Wadt, W. R.; Hay, P. J. *J. Chem. Phys.* **1985**, *82*, 299−310.
(56) Klamt, A.; Jonas, V.; Buerger, T.; Lohrenz, J. C. W. *J. Phys. Chem.* **1998**, *102*, 5074−5085.
(57) Glendening, E. D.; Reed, A. E.; Carpenter, J. E.; Weinhold, F. *NBO*, version 3.1; Theoretical Chemistry Institute, University of Wisconsin: Madison, WI, 1996.
(58) Marenich, A. V.; Cramer, C. J.; Truhlar, D. G. *J. Phys. Chem. B* **2009**, *113*, 6378−6396.
(59) Biedermann, F.; Scherman, O. A. *J. Phys. Chem. B* **2012**, *116*, 2842−2849.
(60) Sundararajan, M.; Ghosh, S. K. *J. Inclusion Phenom. Macrocyclic Chem.* **2012**, *72*, 437−441.
(61) Peerannawar, S. R.; Gobre, V. V.; Gejji, S. P. *Comput. Theor. Chem.* **2011**, *966*, 154−158.
(62) Ma, D.; Hettiarachchi, G.; Nguyen, D.; Zhang, B.; Wittenberg, J. B.; Zavalij, P. Y.; Briken, V.; Lsaacs, L. *Nat. Chem.* **2012**, *4*, 503−510.
(63) Lei, W. H.; Zhou, Q. X.; Jiang, G. Y.; Hou, Y. J.; Zhang, B. W.; Cheng, X. X.; Wang, X. S. *Chem. Phys. Chem.* **2011**, *12*, 2933−2940.
(64) Biedermann, F.; Uzunova, V. D.; Scherman, O. A.; Nau, W. M.; Simone, A. D. *J. Am. Chem. Soc.* **2012**, *134*, 15318−15323.
(65) Bardelang, D.; Udachin, K. A.; Leek, D. M.; Margeson, J. C.; Chan, G.; Ratcliffe, C. I.; Ripmeester, J. A. *Cryst. Growth Des.* **2011**, *11*, 5598−5614.